

Article

Interaction between the L-Ascorbic Acid and the HO₂ Hydroperoxyl Radical: An Ab Initio Study

Iván Carrillo Díaz^{1,2}, Ali Fransuani Jiménez González² , Juan Manuel Ramírez-de-Arellano^{1,*} 
and Luis Fernando Magaña² 

¹ Tecnológico de Monterrey, Escuela de Ingeniería y Ciencias, Calle del Puente 222, Mexico City 14380, Mexico; icarrillodiaz@tec.mx

² Instituto de Física, Universidad Nacional Autónoma de México, Mexico City 01000, Mexico; alifransuanijg@gmail.com (A.F.J.G.); fernando@fisica.unam.mx (L.F.M.)

* Correspondence: jramirezdearellano@tec.mx

Abstract: We studied the interaction between the L-ascorbic acid C₆H₈O₆ and the HO₂ hydroperoxyl radical, using DFT ab initio methods. The purpose of this study is to explore whether the L-ascorbic acid would be able to interact with and possibly reduce the hydroperoxyl radical. We performed static calculations consisting of structural optimizations, using the pseudopotential formalism and the LDA, PBE, and BLYP density functional approximations, including van der Waals corrections. For all the cases considered, we found an interaction between C₆H₈O₆ and HO₂, reporting recovery times and absorption energies consistent with a physisorption process and confirming the ability of the L-ascorbic acid to act as a sensor of the HO₂ radical.

Keywords: DFT; absorption; hydroperoxyl



Citation: Carrillo Díaz, I.; Jiménez González, A.F.; Ramírez-de-Arellano, J.M.; Magaña, L.F. Interaction between the L-Ascorbic Acid and the HO₂ Hydroperoxyl Radical: An Ab Initio Study. *Crystals* **2023**, *13*, 1135. <https://doi.org/10.3390/cryst13071135>

Academic Editor: Sławomir Grabowski

Received: 17 June 2023
Revised: 12 July 2023
Accepted: 17 July 2023
Published: 20 July 2023



Copyright: © 2023 by the authors. Licensee MDPI, Basel, Switzerland. This article is an open access article distributed under the terms and conditions of the Creative Commons Attribution (CC BY) license (<https://creativecommons.org/licenses/by/4.0/>).

1. Introduction

Free radicals—or simply radicals—are ions, atoms, or molecules with unpaired electrons, a feature that usually makes them highly reactive, as they try to capture an electron from other atoms to stabilize themselves [1]. When they achieve this, they start a chain reaction that generates more radicals. Though necessary for life, evidence shows that these radicals, particularly superoxide or hydrogen peroxide, can produce oxidative damage to living beings, which may be one cause for cellular aging [2,3].

L-ascorbic acid, or Vitamin C (C₆H₈O₆), is an antioxidant substance that may deter the propagation and proliferation of free radicals, transforming them into inert radicals or oxidizing itself. L-ascorbic acid is soluble in water and occurs naturally in different foods—particularly fruits and vegetables—and beverages, as well as being available as a supplement [4]. An intake of 40–110 mg/day is recommended by different national agencies around the world [4,5]. Considering that the human body is unable to produce Vitamin C by itself [6], several studies have focused on the role that such intake might have in preventing or treating cancer, cardiovascular disease, age-related macular degeneration, and the common cold [7–11]. On the other hand, it is well-documented that the deficiency of L-ascorbic acid causes scurvy [12,13].

The structure, molecular force field, and different properties of L-ascorbic acid have been previously studied both experimentally and using DFT methods [14], both in the solid state and considering an aqueous solution. Other studies have also provided insights into the interaction between L-ascorbic acid and different radicals. For instance, it has been shown that ascorbic acid can be oxidized by losing one electron at a time and that disproportionation of the intermediate radical is thermodynamically favored at physiological pH [15]. Ascorbic acid may interact with the plasma membrane by donating electrons to the α -tocopheroxyl radical, and transplasma membrane oxidoreductase activity [16]. Other studies show that hydrogen oxoperoxonitrate oxidizes monohydrogen L-ascorbate

by one electron [17]. And others have focused on the stability and surface properties of L-ascorbic acid alkyl esters and their differential interaction with lipid membranes [18]. Overall, the literature suggests that L-ascorbic acid can interact with free radicals and other species [19], but further studies are needed to fully understand the mechanisms and physiological significance of these interactions.

In an effort to contribute to the literature in that direction, in this work, we study the interaction between the L-ascorbic acid and the hydroperoxyl free radical (HO_2), also known as hydrogen superoxide. This radical is formed by the transfer of an H atom onto molecular oxygen. Due to its high reactivity, it acts as an oxidant agent in different biological processes [20]. Understanding the possible interactions between these two substances is relevant to the development of health and safety solutions regarding the action of free radicals in biological systems.

2. Materials and Methods

We performed ab initio calculations using density functional theory (DFT) methods [21,22], within the Born–Oppenheimer approximation [23,24]. The calculations were performed using the code suite Quantum ESPRESSO, an open-source tool that considers plane waves for the basis set, and periodic boundary conditions [25–27]. We used Troullier–Martins norm-conserving pseudopotentials in the Kleinman–Bylander fully separable form [28,29]. For the exchange and correlation energies, we considered the following density functional approximations: Perdew–Zunger (LDA) [30], Perdew–Burke–Ernzerhof [31,32], and the hybrid BLYP functional [33,34]. For the PBE and BLYP functionals, we also considered the additional semiempirical Grimme’s DFT-D3 van der Waals correction [35].

The valence electronic states were taken as follows: for hydrogen, $1s$; for carbon, $2s^2 2p^2$; and for oxygen: $2s^2 2p^4$. The cut-off radii for the pseudopotentials considered are as follows: for hydrogen: $r_s = 0.423 \text{ \AA}$; for carbon: $r_s = 0.794 \text{ \AA}$ and $r_p = 0.815 \text{ \AA}$; and for oxygen: $r_s = r_p = 0.661 \text{ \AA}$, with the s pseudo potential as the local component for all cases.

Non-relativistic, spin-polarized, and non-spin-polarized calculations were performed. The results were the same for both spin-polarized and non-polarized calculations, implying a nonmagnetic system. In this work, we report the non-polarized calculations for that reason. Several ab initio studies have been performed to study the HO_2 radical structure and thermodynamic properties [36,37], and the spin effects on them [38], particularly to calculate in a precise way the formation enthalpies of said radical, when using the HLCC theory, based on the use of molecular orbitals. The influence of spin polarization is important when using molecular orbitals for solving the Kohn–Sham equations, as shown in [39], which focused on studying spin trapping and the influence in the single-point energies of all stationary points. However, the calculation of such properties lies outside of the scope of this work, as we are considering the use of cut-off radii for the plane-wave basis set used, rather than molecular orbitals. This could explain the equivalent results for both spin- and non-spin-polarized systems in our calculations.

The cut-off energy was set to 1200 eV or 88 Ry, and we considered a $5 \times 5 \times 5$ k-points mesh, within the Monkhorst–Pack special k-point scheme [40]. The threshold energy convergence was 1.1×10^{-5} eV.

The structural relaxations performed are static calculations that correspond to the calculation option ‘relax’ in the Quantum ESPRESSO input file, and they consider a vacuum around the samples.

The absorption energies reported in this work were calculated using the following expression [41]:

$$E_{\text{adsorption}} = E_{\text{system 1+system 2}} - E_{\text{system 1}} - E_{\text{system 2}} \quad (1)$$

In Equation (1), the first term on the right side corresponds to the total energy of the compound system, which, here, refers to the final configuration of the system involving both the L-ascorbic acid and the HO_2 radical. The second and third terms on the right side

of Equation (1) correspond to the total energies of the L-ascorbic acid on one hand, and the HO₂ radical on the other, after being structurally relaxed separately.

We also calculated the corresponding recovery times for each case, a concept that is helpful for estimating the absorption time of the radical on the L-ascorbic acid. This is based on Eyring's theory of state transitions, and can be calculated as [42,43]:

$$\tau = \left(\frac{h}{K_B T} \right) e^{-E_{ads}/K_B T} \quad (2)$$

where E_{ads} is the adsorption energy of HO₂ on the C₆H₈O₆ molecule, and K_B and h are the Boltzmann and Planck's constant, respectively. Recovery times are calculated for the static geometrical optimizations, and the temperature is set at $T = 300$ K in Equation (2) for all cases, although no molecular dynamics calculations are reported in this work.

3. Results

3.1. Structure Optimization

We first performed structural optimizations on the L-ascorbic acid and hydroperoxyl structures separately, to assess the validity of the pseudopotentials and XC-functionals used in this work. As we mentioned earlier, Quantum ESPRESSO considers periodic boundary conditions, and, for this reason, we placed each system at the center of a cubic unit cell with sides 20 Å long. In this way, we avoid spurious interactions between the system and its periodical repetitions.

The initial crystallographic structure for the L-ascorbic acid molecule, or C₆H₈O₆, was obtained through the Crystallography Open Database [44–52], in particular, considering COD-ID Nr. 2300646 [53]. As we were interested in the interaction between one L-ascorbic acid molecule and the HO₂ radical, we used the corresponding co-ordinates for one molecule among the several included in the COD file. Figure 1 shows the L-ascorbic acid molecule obtained in this way, after a structural relaxation is performed on it. In that figure, the labelling has been chosen to be consistent with the one used in previous DFT studies [14]. Table 1 shows the final bond distances obtained for this molecule after being optimized. Table 2 shows the corresponding angles. Similar geometrical relaxations were also performed on the hydroperoxyl radical HO₂, shown in Figure 2. Table 3 summarizes the results of such optimizations, compared with the experimental values as reported in [54], which we used directly to build the initial hydroperoxyl structure. In both cases (C₆H₈O₆ and HO₂), calculations were made considering the following density functional approximations: LDA PZ, PBE, PBE + vdW, BLYP, and BLYP + vdW, where 'vdW' refers to the van der Waals correction previously mentioned. Overall, there is a good agreement with the experimental values (see [54,55]), with the PBE + vdW approximation being more accurate, as expected. The final structures obtained are qualitatively quite similar for all cases, but, for simplicity, in Figures 1 and 2, only those obtained with the PBE-vdW approximation are shown.

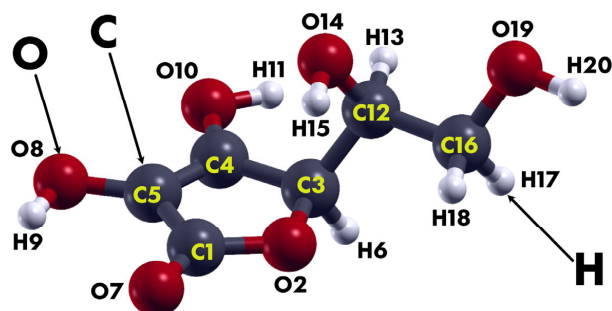


Figure 1. The structure of the L-ascorbic acid (C₆H₈O₆) as considered in this work. It consists of 20 atoms, 6 carbon atoms, 6 oxygen atoms, and 8 hydrogen atoms. The atoms are labeled to identify bond lengths and angles, following the setup used in [14]. This configuration corresponds to the final structure obtained by using the PBE + vdW functional.

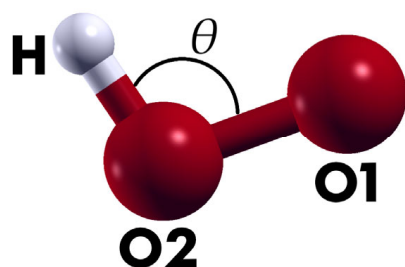


Figure 2. Structure considered in this work for the hydroperoxyl radical HO₂ or HOO. The experimental bond length between the H atom and the O atom (labeled O₂–H) is 0.96 Å, while the bond length between O atoms is equal to 1.3 Å. The angle θ is experimentally equal to 108° (see [54]). The labels correspond to the length and angle identification of Table 3. The figure shows the optimized structure obtained by using the PBE + vdW functional, as in Figure 1.

Table 1. Values of bond lengths (Å) obtained after a structural relaxation (using different density functional approximations) for the L-ascorbic acid, and their corresponding experimental values in the last column (see [55]). The atom labelling corresponds to that of Figure 1, following the labelling structure used in [14].

Parameter	LDA	PBE	PBE + vdW	BLYP	BLYP + vdW	Exp. [55]
C1–O7	1.207	1.215	1.214	1.216	1.215	1.216
C5–O8	1.332	1.352	1.352	1.362	1.362	1.361
C4–O10	1.330	1.350	1.349	1.360	1.359	1.326
C1–O2	1.370	1.389	1.389	1.401	1.401	1.355
C3–O2	1.425	1.446	1.446	1.461	1.461	1.444
C12–O14	1.393	1.415	1.415	1.428	1.429	1.427
C16–O19	1.400	1.424	1.424	1.439	1.439	1.431
C4–C5	1.343	1.350	1.350	1.350	1.350	1.338
C1–C5	1.442	1.456	1.457	1.462	1.463	1.452
C3–C4	1.489	1.504	1.504	1.512	1.510	1.493
C3–C12	1.520	1.544	1.543	1.553	1.552	1.521
C12–C16	1.509	1.530	1.530	1.539	1.538	1.521

Table 2. Values of bond angles (°) obtained after a structural relaxation (using different density functional approximations) for the L-ascorbic acid, and their corresponding experimental values (see [55]). As in Table 1, the labelling setup is based on [14].

Parameter	LDA	PBE	PBE + vdW	BLYP	BLYP + vdW	Exp. [55]
C3–O2–C1	108.4	108.5	108.5	108.6	108.5	109.1
O2–C1–C5	109.5	109.1	109.1	108.7	108.7	109.5
C1–C5–C4	108.1	108.5	108.5	108.9	108.9	107.8
C5–C4–C3	108.6	108.9	108.9	109.3	109.3	109.5
C4–C3–O2	105.4	104.9	105.0	104.4	104.6	104.0
O2–C1–O7	123.9	123.1	123.1	123.0	122.9	121.4
O7–C1–C5	126.6	127.8	127.8	128.3	128.4	129.1
C1–C5–O8	120.1	121.5	121.6	121.8	122.0	124.6
O8–C5–C4	131.8	130.0	129.9	129.3	129.2	127.5
C5–C4–O10	128.0	126.9	126.9	126.4	126.6	133.5
C3–C4–O10	123.4	124.2	124.1	124.3	124.0	117.1
O2–C3–C12	108.0	108.7	108.6	109.1	108.7	114.8
C4–C3–C12	114.2	115.5	115.1	115.9	115.1	110.4
C3–C12–C16	110.2	110.6	110.6	110.9	110.9	111.7
C3–C12–O14	110.8	111.8	111.6	112.0	111.5	112.7
O14–C12–C16	113.2	113.3	113.3	113.2	113.0	106.9
C12–C16–O19	108.3	108.3	108.1	108.1	107.8	108.0

Table 3. Values of bond lengths (Å)—first two rows—and angle (°) after structural relaxations (using the LDA and GGA approximations) for the HO₂ hydroperoxyl radical, and their corresponding experimental values (see [54]). The atom labelling corresponds to that of Figure 2.

Parameter	LDA	GGA	PBE + vdW	BLYP	BLYP + vdW	Exp. [54]
O1–O2	1.320	1.343	1.343	1.333	1.363	1.3
O2–H	0.993	0.989	0.988	0.971	0.989	0.96
H–O2–O1	106.0	105.1	105.2	104.3	104.8	108

3.2. Interaction between C₆H₈O₆ and HO₂: Structural Relaxations in a Vacuum

We first performed a structural relaxation in a vacuum, considering the HO₂ radical at an initial vertical distance of 1.67 Å of the L-ascorbic acid C₆H₈O₆, with respect to the plane that contains its pentagon. Two cases were considered, corresponding to the initial position of the H-atom in the hydroperoxyl radical, either pointing upwards (case 1) or downwards (case 2), with the C₆H₈O₆ pentagon taken as reference. In both cases, the O-atoms axis of the radical is placed parallel to the C₆H₈O₆ pentagon plane. Figure 1 shows the results for case 1.

In that case, the structural relaxation shows an increase in the distance between the HO₂ radical and the C₆H₈O₆, for all density functional approximations considered. In the LDA case, we observe a dissociation of one H-atom from the C₆H₈O₆ onto the radical, something that is not present for the rest of the functionals considered, but, in all cases, the radical stabilizes around the distance shown in Figure 1, until convergence is achieved. Table 4 summarizes the absorption energies and recovery times obtained for the five structural relaxations performed. The results in this section are consistent among themselves, except for the case of the LDA functional, which overestimates the absorption energy, resulting in a rather large value for the recovery time.

The structural relaxation results corresponding to case 2—with the H-atom of the HO₂ radical pointing downward—are shown in Figure 4, which qualitatively shows a similar behavior as case 1. Quantitatively, the final vertical distances in this case are smaller than the previous case. Table 5 shows the corresponding absorption energies and recovery times for calculations corresponding to case 2. We found reasonable values of those parameters when considering the PBE, PBE + vdW, and, to some extent, BLYP + vdW, in terms of sensor developing.

Table 4. Case 1 adsorption energies E_{ads} (in eV) and recovery times (in s) for the interaction between the HO₂ radical and the L-ascorbic acid molecule, using different density functional approximations (see Figure 3). Calculations were structural relaxations in a vacuum.

Density Functional Approximation	E_{ads}	τ
LDA	−1.81	3.83×10^{17}
PBE	−0.43	2.31×10^{-6}
PBE + vdW	−0.36	1.82×10^{-7}
BLYP	−0.31	2.97×10^{-8}
BLYP + vdW	−0.44	4.59×10^{-6}

Table 5. Case 2 adsorption energies E_{ads} (in eV) and recovery times (in s) for the interaction between the HO₂ radical and the L-ascorbic acid molecule, using different density functional approximations (see Figure 3). Calculations were structural relaxations in a vacuum.

Density Functional Approximation	E_{ads}	τ
LDA	−1.33	3.35×10^9
PBE	−0.78	2.09
PBE + vdW	−0.73	0.329
BLYP	−0.17	1.18×10^{-10}
BLYP + vdW	−0.61	3.24×10^{-3}

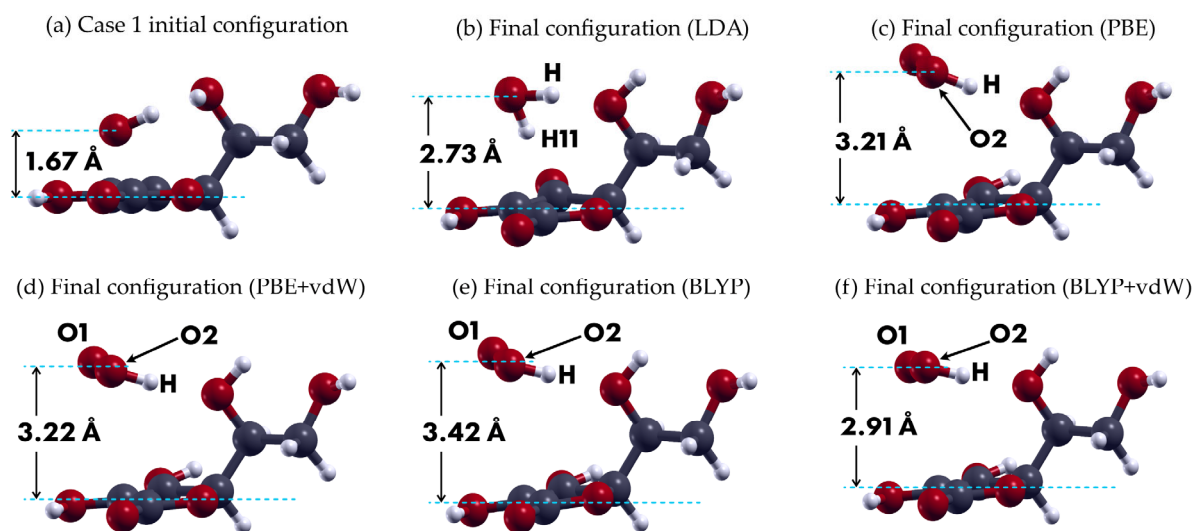


Figure 3. Structural relaxations for the first case considered in this work, corresponding to the H-atom of the radical pointing upward. (a) Initial position: the O-atoms axis is placed parallel to the $C_6H_8O_6$ pentagon plane. The rest of the images in this figure are shown from this same point of view and present the final configurations obtained with (b) the LDA, (c) PBE, (d) PBE + vdW, (e) BLYP, and (f) BLYP + vdW density functional approximations.

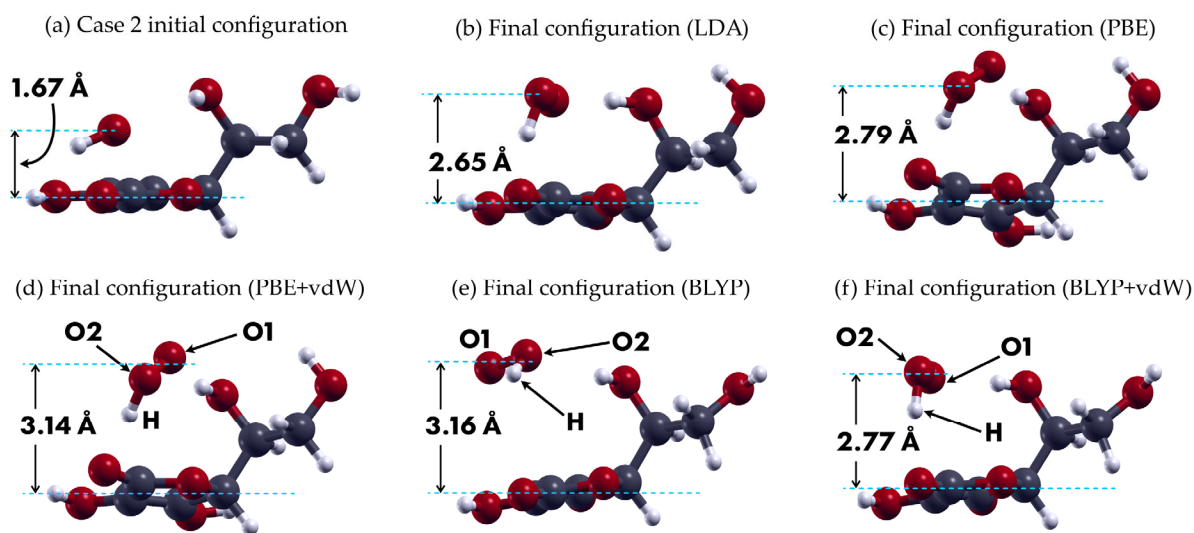


Figure 4. Structural relaxations for the second case considered in this work, corresponding to the H-atom of the radical pointing downward. (a) Initial position: the O-atoms axis is placed parallel to the $C_6H_8O_6$ pentagon plane. The rest of the images in this figure are shown from this same point of view and present the final configurations obtained with (b) the LDA, (c) PBE, (d) PBE + vdW, (e) BLYP, and (f) BLYP + vdW density functional approximations. In both cases, the qualitative behavior is similar to those of case 1.

4. Discussion

The structural relaxations performed on both substances considered in this work resulted in bond distances and angles in good agreement with the experimental values. We used the LDA, PBE, PBE + vdW, BLYP, and BLYP + vdW density functional approximations in this work mainly to confirm the qualitative nature of the interaction studied, which was similar for all functionals considered. The use of different functionals improves the reliability of the results obtained and allows us to focus on the quantitative results corresponding to the functionals known to be more precise. In this case, PBE + vdW gave

the most accurate results in terms of geometry and structure, when compared with the experimental parameters of the systems considered.

We found that the HO₂ radical interacts in all cases with the L-ascorbic acid, which can be assessed as a physisorption in terms of the absorption energy values, according to the structural relaxations performed. Here, we are considering the typical binding energies for chemisorption to be above 0.5 eV per atom (see [41], page 195), and, under that criterion, we conclude that the interaction would rather be a physisorption, even at room temperature, according to the results obtained using the PBE + vW functional.

The absorption energies for case 2—in which the H atom of the radical points initially downward—are consistently larger than those for case 1, particularly when the van der Waals correction is included. This correction allows us to notice the action of the OH bonds from the acid molecule, in the interaction with the H-atom of the radical.

In all cases, the H-atom from the free radical interacts with an oxygen atom of the L-ascorbic acid molecule. The corresponding recovery times, calculated using Equation (2), suggest that L-ascorbic acid could properly detect the presence of the hydroperoxyl radical at room temperature, as suggested by the results using the PBE and PBE + vdW functionals in case 2. There, we obtained absorption energies of −0.78 eV and −0.73 eV, and recovery times of 2.09 and 0.329 s, respectively. The double binding located in the pentagon of the L-ascorbic acid can be considered as a stable reaction site, although we did not find a reduction process of the HO₂ radical.

Author Contributions: Conceptualization, I.C.D., J.M.R.-d.-A. and L.F.M.; data curation, I.C.D., A.F.J.G. and J.M.R.-d.-A.; formal analysis, A.F.J.G., J.M.R.-d.-A. and L.F.M.; funding acquisition, I.C.D., J.M.R.-d.-A. and L.F.M.; investigation, A.F.J.G., J.M.R.-d.-A. and L.F.M.; methodology, A.F.J.G. and J.M.R.-d.-A.; project administration, J.M.R.-d.-A. and L.F.M.; supervision, L.F.M.; validation, I.C.D., A.F.J.G., J.M.R.-d.-A. and L.F.M.; writing—original draft, I.C.D. and J.M.R.-d.-A.; writing—review and editing, A.F.J.G., J.M.R.-d.-A. and L.F.M. All authors have read and agreed to the published version of the manuscript.

Funding: Dirección General de Asuntos del Personal Académico de la Universidad Nacional Autónoma de México (DGAPA-UNAM), by grant number IN102323. The APC was funded by Tecnológico de Monterrey.

Data Availability Statement: Data unavailable due to privacy restrictions.

Acknowledgments: We thank (DGAPA-UNAM) for partial financial support by grant number IN102323. We also appreciate UNAM-Miztli-Super-Computing Center's technical assistance by the project LANCADUNAM-DGTIC-030.

Conflicts of Interest: The authors declare no conflict of interest.

References

1. Hayyan, M.; Hashim, M.A.; AlNashef, I.M. Superoxide Ion: Generation and Chemical Implications. *Chem. Rev.* **2016**, *116*, 3029–3085. [CrossRef] [PubMed]
2. Halliwell, B. Free Radicals and Antioxidants: Updating a Personal View. *Nutr. Rev.* **2012**, *70*, 257–265. [CrossRef] [PubMed]
3. Halliwell, B.; Gutteridge, J.M.C. *Free Radicals in Biology and Medicine*; Oxford University Press: Oxford, UK, 2015; ISBN 978-0-19-871747-8.
4. Panel on Dietary Antioxidants and Related Compounds; Subcommittee on Upper Reference Levels of Nutrients; Subcommittee on Interpretation and Uses of Dietary Reference Intakes; Standing Committee on the Scientific Evaluation of Dietary Reference Intakes; Food and Nutrition Board; Institute of Medicine. *Dietary Reference Intakes for Vitamin C, Vitamin E, Selenium, and Carotenoids*; National Academies Press: Washington, DC, USA, 2000; p. 9810, ISBN 978-0-309-06935-9.
5. World Health Organization. *Vitamin and Mineral Requirements in Human Nutrition*, 2nd ed.; World Health Organization: Geneva, Switzerland; FAO: Rome, Italy, 2004; ISBN 978-92-4-154612-6.
6. Paasch, S.; Salzer, R. Solution to Spectroscopy Challenge 7. *Anal. Bioanal. Chem.* **2004**, *380*, 734–735. [CrossRef] [PubMed]
7. Office of Dietary Supplements Vitamin, C. Fact Sheet for Health Professionals. Available online: <https://ods.od.nih.gov/factsheets/VitaminC-HealthProfessional/> (accessed on 16 June 2023).
8. Li, Y.; Schellhorn, H.E. New Developments and Novel Therapeutic Perspectives for Vitamin C. *J. Nutr.* **2007**, *137*, 2171–2184. [CrossRef]

9. Carr, A.C.; Frei, B. Toward a New Recommended Dietary Allowance for Vitamin C Based on Antioxidant and Health Effects in Humans. *Am. J. Clin. Nutr.* **1999**, *69*, 1086–1107. [[CrossRef](#)]
10. Honarbakhsh, S.; Schachter, M. Vitamins and Cardiovascular Disease. *Br. J. Nutr.* **2008**, *101*, 1113–1131. [[CrossRef](#)]
11. Jacobs, C.; Hutton, B.; Ng, T.; Shorr, R.; Clemons, M. Is There a Role for Oral or Intravenous Ascorbate (Vitamin C) in Treating Patients With Cancer? A Systematic Review. *Oncologist* **2015**, *20*, 210–223. [[CrossRef](#)]
12. Wang, A.H.; Still, C. Old World Meets Modern: A Case Report of Scurvy. *Nutr. Clin. Pract.* **2007**, *22*, 445–448. [[CrossRef](#)]
13. Stephen, R.; Utecht, T. Scurvy Identified in the Emergency Department: A Case Report. *J. Emerg. Med.* **2001**, *21*, 235–237. [[CrossRef](#)]
14. Bichara, L.C.; Lanús, H.E.; Nieto, C.G.; Brandán, S.A. Density Functional Theory Calculations of the Molecular Force Field of L-Ascorbic Acid, Vitamin C. *J. Phys. Chem. A* **2010**, *114*, 4997–5004. [[CrossRef](#)]
15. Tu, Y.-J.; Njus, D.; Schlegel, H.B. A Theoretical Study of Ascorbic Acid Oxidation and $\text{HOO}^\cdot/\text{O}_2^{\cdot-}$ Radical Scavenging. *Org. Biomol. Chem.* **2017**, *15*, 4417–4431. [[CrossRef](#)]
16. May, J.M. Is Ascorbic Acid an Antioxidant for the Plasma Membrane? *FASEB J.* **1999**, *13*, 995–1006. [[CrossRef](#)]
17. Bartlett, D.; Church, D.F.; Bounds, P.L.; Koppenol, W.H. The Kinetics of the Oxidation of L-Ascorbic Acid by Peroxynitrite. *Free Radic. Biol. Med.* **1995**, *18*, 85–92. [[CrossRef](#)]
18. Mottola, M.; Vico, R.V.; Villanueva, M.E.; Fanani, M.L. Alkyl Esters of L-Ascorbic Acid: Stability, Surface Behaviour and Interaction with Phospholipid Monolayers. *J. Colloid Interface Sci.* **2015**, *457*, 232–242. [[CrossRef](#)]
19. Sharma, M.K.; Buettner, G.R. Interaction of Vitamin C and Vitamin E during Free Radical Stress in Plasma: An ESR Study. *Free Radic. Biol. Med.* **1993**, *14*, 649–653. [[CrossRef](#)]
20. De Grey, A.D.N.J. HO_2^\cdot : The Forgotten Radical. *DNA Cell Biol.* **2002**, *21*, 251–257. [[CrossRef](#)]
21. Cottenier, S. *Density Functional Theory and the Family of (L)APW-Methods: A Step-by-Step Introduction*, 2nd ed.; Center for Molecular Modeling (CMM) & Department of Materials Science and Engineering (DMSE) Ghent University: Ghent, Belgium, 2013.
22. Parr, R.G.; Yang, W. *Density-Functional Theory of Atoms and Molecules*; International Series of Monographs on Chemistry; Oxford University Press: Oxford, UK; Clarendon Press: New York, NY, USA, 1989; ISBN 978-0-19-504279-5.
23. Marx, D.; Hutter, J. *Ab Initio Molecular Dynamics: Basic Theory and Advanced Methods*, 1st ed.; Cambridge University Press: Cambridge, UK, 2012; ISBN 978-1-107-66353-4.
24. Born, M.; Oppenheimer, R. Zur Quantentheorie der Molekeln. *Ann. Phys.* **1927**, *389*, 457–484. [[CrossRef](#)]
25. Giannozzi, P.; Andreussi, O.; Brumme, T.; Bunau, O.; Buongiorno Nardelli, M.; Calandra, M.; Car, R.; Cavazzoni, C.; Ceresoli, D.; Cococcioni, M.; et al. Advanced Capabilities for Materials Modelling with Quantum ESPRESSO. *J. Phys. Condens. Matter* **2017**, *29*, 465901. [[CrossRef](#)]
26. Giannozzi, P.; Baroni, S.; Bonini, N.; Calandra, M.; Car, R.; Cavazzoni, C.; Ceresoli, D.; Chiarotti, G.L.; Cococcioni, M.; Dabo, I.; et al. QUANTUM ESPRESSO: A Modular and Open-Source Software Project for Quantum Simulations of Materials. *J. Phys. Condens. Matter* **2009**, *21*, 395502. [[CrossRef](#)]
27. Giannozzi, P.; Baseggio, O.; Bonfà, P.; Brunato, D.; Car, R.; Carnimeo, I.; Cavazzoni, C.; de Gironcoli, S.; Delugas, P.; Ferrari Ruffino, F.; et al. QUANTUM ESPRESSO toward the Exascale. *J. Chem. Phys.* **2020**, *152*, 154105. [[CrossRef](#)]
28. Troullier, N.; Martins, J. A Straightforward Method for Generating Soft Transferable Pseudopotentials. *Solid State Commun.* **1990**, *74*, 613–616. [[CrossRef](#)]
29. Kleinman, L.; Bylander, D.M. Efficacious Form for Model Pseudopotentials. *Phys. Rev. Lett.* **1982**, *48*, 1425–1428. [[CrossRef](#)]
30. Perdew, J.P.; Zunger, A. Self-Interaction Correction to Density-Functional Approximations for Many-Electron Systems. *Phys. Rev. B* **1981**, *23*, 5048–5079. [[CrossRef](#)]
31. Perdew, J.P.; Burke, K.; Ernzerhof, M. Generalized Gradient Approximation Made Simple. *Phys. Rev. Lett.* **1996**, *77*, 3865–3868. [[CrossRef](#)] [[PubMed](#)]
32. Perdew, J.P.; Burke, K.; Ernzerhof, M. Generalized Gradient Approximation Made Simple [Phys. Rev. Lett. 77, 3865 (1996)]. *Phys. Rev. Lett.* **1997**, *78*, 1396. [[CrossRef](#)]
33. Becke, A.D. Density-Functional Exchange-Energy Approximation with Correct Asymptotic Behavior. *Phys. Rev. A* **1988**, *38*, 3098–3100. [[CrossRef](#)]
34. Lee, C.; Yang, W.; Parr, R.G. Development of the Colle-Salvetti Correlation-Energy Formula into a Functional of the Electron Density. *Phys. Rev. B* **1988**, *37*, 785–789. [[CrossRef](#)]
35. Grimme, S.; Antony, J.; Ehrlich, S.; Krieg, H. A Consistent and Accurate Ab Initio Parametrization of Density Functional Dispersion Correction (DFT-D) for the 94 Elements H-Pu. *J. Chem. Phys.* **2010**, *132*, 154104. [[CrossRef](#)]
36. Liskow, D.H.; Schaefer, H.F.; Bender, C.F. Geometry and Electronic Structure of the Hydroperoxyl Radical. *J. Am. Chem. Soc.* **1971**, *93*, 6734–6737. [[CrossRef](#)]
37. Flowers, B.A.; Szalay, P.G.; Stanton, J.F.; Kállay, M.; Gauss, J.; Császár, A.G. Benchmark Thermochemistry of the Hydroperoxyl Radical. *J. Phys. Chem. A* **2004**, *108*, 3195–3199. [[CrossRef](#)]
38. Bil, A.; Latajka, Z. The Hydroperoxy Radical and Its Closed-Shell ‘analogues’: Ab Initio Investigations. *Chem. Phys. Lett.* **2004**, *388*, 158–163. [[CrossRef](#)]
39. Durand, G.; Choteau, F.; Pucci, B.; Villamena, F.A. Reactivity of Superoxide Radical Anion and Hydroperoxyl Radical with α -Phenyl-*N-Tert*-Butylnitron (PBN) Derivatives. *J. Phys. Chem. A* **2008**, *112*, 12498–12509. [[CrossRef](#)] [[PubMed](#)]
40. Monkhorst, H.J.; Pack, J.D. Special Points for Brillouin-Zone Integrations. *Phys. Rev. B* **1976**, *13*, 5188–5192. [[CrossRef](#)]

41. Oura, K. (Ed.) *Surface Science: An Introduction*; Advanced Texts in Physics; Springer: Berlin/Heidelberg, Germany; New York, NY, USA, 2003; ISBN 978-3-540-00545-2.
42. Eyring, H. The Activated Complex in Chemical Reactions. *J. Chem. Phys.* **1935**, *3*, 107–115. [[CrossRef](#)]
43. Popa, I.; Fernández, J.M.; Garcia-Manyes, S. Direct Quantification of the Attempt Frequency Determining the Mechanical Unfolding of Ubiquitin Protein. *J. Biol. Chem.* **2011**, *286*, 31072–31079. [[CrossRef](#)]
44. Downs, R.T.; Hall-Wallace, M. The American Mineralogist Crystal Structure Database. *Am. Mineral.* **2003**, *88*, 247–250.
45. Gražulis, S.; Chateigner, D.; Downs, R.T.; Yokochi, A.F.T.; Quirós, M.; Lutterotti, L.; Manakova, E.; Butkus, J.; Moeck, P.; Le Bail, A. Crystallography Open Database—An Open-Access Collection of Crystal Structures. *J. Appl. Crystallogr.* **2009**, *42*, 726–729. [[CrossRef](#)]
46. Gražulis, S.; Daškevič, A.; Merkys, A.; Chateigner, D.; Lutterotti, L.; Quirós, M.; Serebryanaya, N.R.; Moeck, P.; Downs, R.T.; Le Bail, A. Crystallography Open Database (COD): An Open-Access Collection of Crystal Structures and Platform for World-Wide Collaboration. *Nucleic Acids Res.* **2012**, *40*, D420–D427. [[CrossRef](#)]
47. Gražulis, S.; Merkys, A.; Vaitkus, A.; Okulič-Kazarinas, M. Computing Stoichiometric Molecular Composition from Crystal Structures. *J. Appl. Crystallogr.* **2015**, *48*, 85–91. [[CrossRef](#)]
48. Le Bail, A. Inorganic Structure Prediction with It GRINSP. *J. Appl. Crystallogr.* **2005**, *38*, 389–395. [[CrossRef](#)]
49. Merkys, A.; Vaitkus, A.; Butkus, J.; Okulič-Kazarinas, M.; Kairys, V.; Gražulis, S. COD::CIF::Parser: An Error-Correcting CIF Parser for the Perl Language. *J. Appl. Crystallogr.* **2016**, *49*, 292–301. [[CrossRef](#)]
50. Merkys, A.; Vaitkus, A.; Grybauskas, A.; Konovalovas, A.; Quirós, M.; Gražulis, S. Graph Isomorphism-Based Algorithm for Cross-Checking Chemical and Crystallographic Descriptions. *J. Cheminform.* **2023**, *15*, 25. [[CrossRef](#)]
51. Quirós, M.; Gražulis, S.; Girdzijauskaitė, S.; Merkys, A.; Vaitkus, A. Using SMILES Strings for the Description of Chemical Connectivity in the Crystallography Open Database. *J. Cheminform.* **2018**, *10*, 23. [[CrossRef](#)]
52. Vaitkus, A.; Merkys, A.; Gražulis, S. Validation of the Crystallography Open Database Using the Crystallographic Information Framework. *J. Appl. Crystallogr.* **2021**, *54*, 661–672. [[CrossRef](#)]
53. McMonagle, C.J.; Probert, M.R. Reducing the Background of Ultra-Low-Temperature X-Ray Diffraction Data through New Methods and Advanced Materials. *J. Appl. Crystallogr.* **2019**, *52*, 445–450. [[CrossRef](#)]
54. Paukert, T.T.; Johnston, H.S. Spectra and Kinetics of the Hydroperoxyl Free Radical in the Gas Phase. *J. Chem. Phys.* **1972**, *56*, 2824–2838. [[CrossRef](#)]
55. Hvoslef, J. The Crystal Structure of L -Ascorbic Acid, ‘vitamin C’. II. The Neutron Diffraction Analysis. *Acta Crystallogr. B* **1968**, *24*, 1431–1440. [[CrossRef](#)]

Disclaimer/Publisher’s Note: The statements, opinions and data contained in all publications are solely those of the individual author(s) and contributor(s) and not of MDPI and/or the editor(s). MDPI and/or the editor(s) disclaim responsibility for any injury to people or property resulting from any ideas, methods, instructions or products referred to in the content.